QRS Complex Detection Based on Primitive

Seungmin Lee, Daejin Park, and Kil Houm Park

Abstract: **The detection of the QRS complex is one of the most important issues in electrocardiogram (ECG) signal analysis. Although research on the detection of the R-peak has demonstrated a high detection rate through a diverse number of studies, research on the detection of the onset and offset boundaries of the QRS complex has proven to be difficult, as the locations of these endpoints are often unclear, and the detection results are difficult to interpret. Hence, detection research through improved algorithms continues to be an important component of the ECG signal analysis, especially given the importance of the QRS complexs role in the diagnosis of arrhythmia through measuring the length of the onset and offset of the QRS complex. This paper proposes an improved algorithm that focuses on the primitive of the QRS complex for detecting the onset and offset of the complex based on the morphological characteristics of the QRS complex. The proposed algorithm was tested through experiments based on QT database (QT-DB) data provided by Physionet, and the outcome revealed not only the reliable detection of the QRS complex boundaries but also results that were superior to the location information recorded in the QT-DB.**

Index Terms: **electrocardiogram (ECG), QRS complex, QRS duration, primitive, QT database (QT-DB)**

I. INTRODUCTION

THE electrocardiogram (ECG) signal is an electrical signal representing the electrical activity of the heart, which is measured from the surface of the body [1]. The steps of the electrical activity of the heart represent the depolarization and re-polarization activities of the atrium and ventricular cells, and are displayed as a continuous waveform of the P-wave, QRS complex, and T-wave [2], [3]. The P-wave, the QRS complex, and the T-wave represent the depolarization of the atrium, the depolarization of the ventricles, and the polarization of the ventricles, respectively, where the intervals, amplitude, shape, etc., of the waveform provide useful information for diagnosing heart disease [4].

The QRS complex is the most prominent characteristic waveform of the ECG signal and is easier to detect than other waveforms are because it has the highest amplitude in each heartbeat period. Generally, the QRS complex is considered a basic step in ECG signal analysis, as the measurement of the heartbeat in beats per minute (BPM) is based on the detection of the QRS complex, and is also the basis of P-wave and T-wave detection. Hence, the QRS complex has been proposed in diverse detection methods, such as QRS type detection in differentiation of ECG signal [5], the Hilbert transform [6], and the Wavelet transform [7].

Significant research related to the detection of the QRS onset and offset boundaries has been conducted [8]–[10]. Given that the width of the QRS complex is an important feature in the diagnosis of arrhythmia, the onset and offset detection of the QRS complex is an essential research component for the automatic classification of arrhythmia. In this respect, the Hilbert transform and Wavelet transform are commonly used to detect the onset and offset of the QRS complex. Moreover, in addition to playing an important role in determining arrhythmia, QRS boundary detection is also useful for compressing the ECG signal at vertex points [11].

In general, the width of the QRS complex is approximately 0.06 to 0.10 s, which varies depending not only on the heart rate of an individual but also on errors generated by different forms of QRS complexes in the individual. Notably, the shape of the QRS complex can vary significantly in the case of measuring arrhythmia. Moreover, due to fluctuations in the baseline of the QRS complex, it is not only difficult to use the value of the amplitude but the process can also generate detection errors due to signal distortions that arise in the process of removing baseline fluctuations. For these reasons, it is difficult to determine the fixed boundaries of the QRS complex and to understand the QRS complex, since an extreme peak, such as the R-peak, is not readily evident.

Therefore, in this paper, we propose a method of detecting a reliable onset and offset of the QRS complex based on the morphological characteristics of the QRS complex by using the primitive of the QRS complex. This method begins with determining the primitive of the QRS complex from the initial normal heartbeat acquired from the input ECG signal. Next, the left and right primitives are separated around the R-peak point from the acquired primitive of the QRS complex. Upon separation, each primitive is horizontally scaled in the search window at a length of 0.05 s given that the normal width of the QRS complex is approximately 0.10 s. For each horizontally scaled primitive, vertical scaling and vertical direction translation are also taken at both ends of the primitive to ensure a proper match between the primitive and the input signal. Finally, after matching the two endpoints for each horizontally scaled primitive and input signal, the average error between the primitive and the input signal is calculated with the smallest average errors at the two detected endpoints as the onset and offset for the scaled primitive.

We propose a simple method to determine the primitive and to efficiently extract the time-voltage information of onset, offset, and peak for given ECG signal so that the ECG signal-aware

Manuscript received July 26, 2016; approved for publication by Yik Chung Wu, Division I Editor, June 7, 2017.

This work was supported by the Institute for Information & communications Technology Promotion(IITP) grant funded by the Korea government(MSIP). [No. 10041145, Self-Organized Software platform(SoSp) for Welfare Devices]. This study was supported by the BK21 Plus project funded by the Ministry of Education, Korea (21A20131600011) and by the Basic Science Research Program through the National Research Foundation of Korea(NRF) funded by the Ministry of Education (2014R1A6A3A04059410 and 201616210000).

The authors are with the School of Electronics Engineering, Kyungpook National University, 80 Daehak-ro, Buk-gu, Daebu, Republic of Korea, email: {lsm1106, boltanut}@knu.ac.kr, khpark@ee.knu.ac.kr.

D. J. Park and K. H. Park are the corresponding authors.

Digital object identifier: 10.1109/JCN.2017.000076

Table 1. Distribution of 105 records of QT-DB.

Provider	Type	Record
MIT-BIH	Arrhyt.	15
MIT-BIH	ST-DB	6
MIT-BIH	Sup. Vent.	13
MIT-BIH	Long Term	4
ESC	STT	33
MIT-BIH	NSR DB	10
Sudden	Death	24

signal processing algorithm can be easily embedded into tiny microcontrollers without transferring raw data of the sampled data for the server-side signal processing. The small set of the fiducial points of the onset, offset, peak positions detected by the proposed algorithm will be only transferred via a wireless interface in wearable devices, which results in the reduction of communication overhead.

The proposed algorithm was derived from experiments conducted with QT-DB data, as provided by PhysioNet. QT-DB provides manually recorded data on waveforms, including the normal sinus rhythm database (NSRD). Based on data from the QT-DB, we were able to confirm the superiority of our proposed algorithm by comparing the clustering diagrams of the QRS complex from the NSRD annotated results with the detected results from our proposed algorithm.

This paper is organized as follows. Section II introduces the QT-DB used in the experiments, including an explanation of the conventional QRS complex detection algorithm. Section III introduces the proposed algorithm, which is the primitive-based QRS onset and offset detection algorithm. Section IV explains the experimental results of the proposed algorithm of QT-DB, and Section V presents our conclusions.

II. REVIEW ON EXISTING METHODS

A. QT Database

ECG morphologies were taken from the QT-DB [12] to account for a wide variety of QRS and ST-T morphologies. The records were primarily chosen from existing ECG databases, including the MIT-BIH Arrhythmia Database [13], the European Society of Cardiology ST-T Database [14] (courtesy of Prof. Carlo Marchesi), and several other ECG databases collected at Boston's Beth Israel Deaconess Medical Center. Notably, the QT-DB was chosen for our experiments due to the diversity and unique aspects of the data within, of which we have added reference annotations marking the locations of waveform boundaries.

Data that did not show significant baseline fluctuations or interference were intentionally selected from the QT-DB, which included a total of 105, fifteen-minute excerpts of two-channel ECGs, as shown in Table 1.

All records were sampled at 250 Hz, and between 30 and 100 representative beats were manually annotated within each record by cardiologists who identified the beginning, peak, and end of the P-wave, QRS complex, T-wave, and U-wave. Based on this annotated information, we were able to evaluate the quality of the algorithm, including the calculated length of the interval or the location information of each record.

B. QRS Complex Detection Method

B.1 Hilbert Transform

Various algorithms have been developed for detecting the QRS complex onset and offset, including the Hilbert transform. In the Hilbert transform algorithm [15], the R-peak is first detected with an algorithm that takes into account the amplitude and the curvature of the ECG signal, to distinguish the R waves from other waves. Subsequently, an auxiliary signal is defined by using the Hilbert transform and differentiation. Equation (1) is the Hilbert transform of the ECG signal.

$$ECG_e(k) = \sqrt{ECG^2(k) + ECG_H^2(k)} \tag{1}$$

$ECG(k)$ is an amplitude of the ECG signal, $ECG_H(k)$ is an amplitude of the imaginary value of the Hilbert transform, and $ECG_e(k)$ is the envelope signal. From (1), the slope of the envelope signal is defined as (2), and the auxiliary signal($AS(k)$) is determined as (3).

$$\begin{aligned} ECG'_e(k) &\approx \frac{1}{10}(2(ECG_e(k+2r) - ECG_e(k-2r)) \\ &+ ECG_e(k+r) - ECG_e(k-r)) \qquad (2) \\ AS(k) &= 2(ECG'_e(k))^2 \qquad (3) \end{aligned}$$

Using an auxiliary signal, two search windows containing the QRS onset and offset are defined. Inside these windows, the detection of the QRS onset and offset is achieved with the aid of a hypothesis test. However, the algorithm using the Hilbert transform produces an error in accordance with an auxiliary signal, which can be distorted by preprocessing algorithms for removing the baseline wandering and reducing noise.

B.2 Wavelet Transform

The wavelet transform can analyze the signal in the time-scale domain and represent the temporal features of a signal at a different resolution. Therefore, it is suitable to use the wavelet transform for analyzing the ECG signal, as it is characterized by the cyclic occurrence of patterns with different frequency waves. Moreover, the noise and artifacts affecting the ECG signal also appear at different frequency bands, thus generating different contributions at various scales. Generally, the wavelet transform of the ECG signal is shown in (4).

$$W_a x(b) = \frac{1}{\sqrt{a}} \int_{-\infty}^{+\infty} x(t)\psi(\frac{t-b}{a})dt \tag{4}$$

a and b denote the dilation and translation factors, respectively, and $\psi(t)$ is a single prototype wavelet. The greater the scale factor a, the wider the basis function; consequently, the corresponding coefficient provides information about lower-frequency components of the signal and vice versa. One of the wavelet transform algorithms using the multi-scale method [7] determines the threshold value for each scale of the given basis function. If the position of sampled signal satisfies these determined threshold values and it can be detected as the zero-crossing point in the first scale, it is treated as the QRS complex. This approach finds out a peak position of QRS with the zero-crossing point, so that this peak point guides to locate onset position before the first significant slope and offset position after

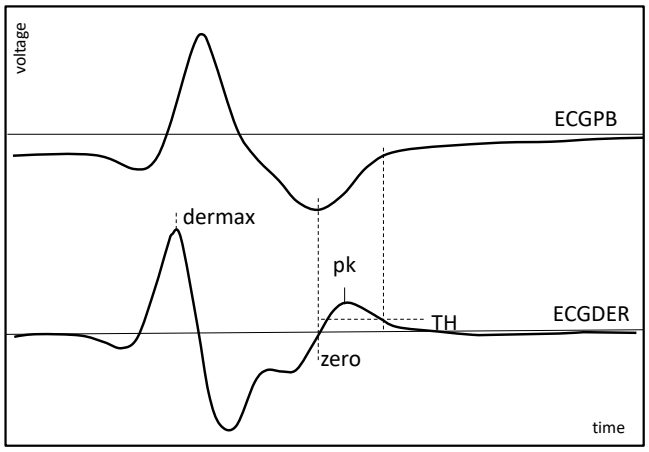

Fig. 1. Determination of the QRS end by the threshold.

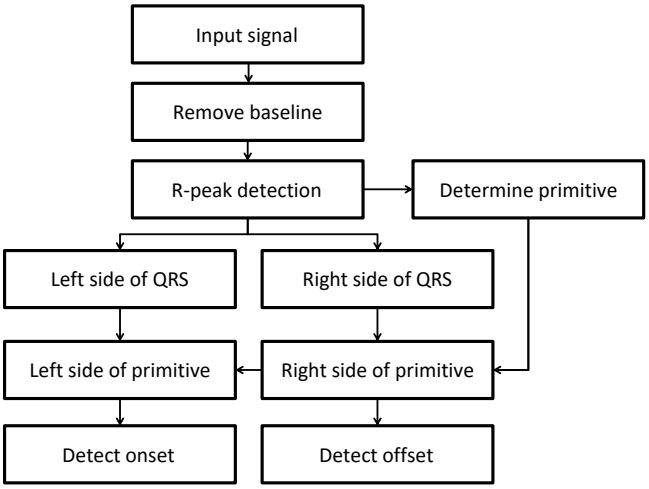

Fig. 2. Proposed algorithm flowchart.

the last significant slope of the QRS, which can be associated with a maximum value of QRS width. A higher reliability of the basis functions means that the performance of the wavelet transform is adequate. However, it is difficult to determine a suitable basis function because the shape of the cyclic pattern, especially the QRS complex, varies, and designating the corresponding threshold is difficult.

B.3 Low-Pass Differentiation

Low-pass differentiation (LPD) [16] makes use of the differentiated ECG signal and information about the wave shape. In an adaptation of differentiation described by Pan and Tompkins [5], the R-peak can be determined as the $QRS_j(i)$ of the position of beat i in lead j. The QRS position given by the detector may be Q, R, or S wave peaks. Thus, the algorithm searches for the nearest zero-crossing position before (p_b) and after (p_a) for the $QRS_j(i)$ position in the differentiated signal (ECGDER) of the band-pass filtered signal (ECGPB). According to the polarity and relative value of these peaks, the algorithm decides if $QRS_j(i)$ belongs to the Q, the R, or the S wave. The adjacent wave positions are detected as the nearest zero-crossing points to $QRS_j(i)$ in ECGDER. The threshold value is experimentally adjusted and is different for Q, R, S, or R' waves, ranging from 3 to 10% of the maximum QRS slope. Fig. 1 shows this procedure for QRS end determination.

From the $zero$ point (S wave position), the algorithm searches for the adjacent peak (pk) on the right (at the end). Using ECGDER(pk), a threshold (TH) is defined as $TH = ECGDER(pk)/k$. Thus, the algorithm determines the end point of the wave as the forward threshold crossing point from $zero$ in the ECGDER signal. Because the value of k is a constant that is experimentally adjusted, it is hard to determine the thresholds, and more errors occur if the number of leads is reduced.

III. PROPOSED METHOD

A. Preprocessing

In general, a number of interference factors can be found in an ECG signal, including the interference of the power supply, noise due to the surface amplitude of baseline fluctuations, and movement of the measurement object. To eliminate these elements and improve the quality of the signal, various preprocessing filters can be employed, such as a finite impulse response (FIR) filter, the empirical mode decomposition (EMD) method, and morphological operations, which helps with the detection of the QRS complex as the R-peak signal becomes relatively stronger.

A key proposition of this paper is that the detection of the QRS complex onset and offset can be determined through the primitive based on improved R-peak detection results. Because the QRS complex is characterized by its repeated nature, the primitive can be determined with respect to the input signal. Moreover, the shape of the primitive can be adaptively converted and matched to detect the QRS complex onset and offset based on the acquired R-peak points. This paper's proposed QRS complex detection process using the primitive is depicted in Fig. 2.

B. Determine Primitive

Fig. 3 depicts the division of the QRS complex into the Q-wave, R-wave, and S-wave of the input signal.

Generally, the starting point of the Q-wave and the ending point of S-wave are defined as the onset and offset of the QRS complex, respectively. As shown in Fig. 3, the area of the QRS complex from the onset to the offset is defined as the primitive for the initially entered QRS complex. Notably, the shape and range of the QRS complex can be identified and detected from the input signal through the primitive. The onset and offset of the QRS complex can also be detected by adaptively matching the primitive.

C. Match Primitive

Scaling is essential for matching the primitive to the QRS complex. The detection process must be based on an optimum scale value of the primitive given that the width of the QRS complex can slightly increase or decrease and that the amplitude value can rise or fall in accordance with an individual's heartbeat. However, due to baseline fluctuations in the ECG signal, the vertical length of the left and right signals is likely to change,

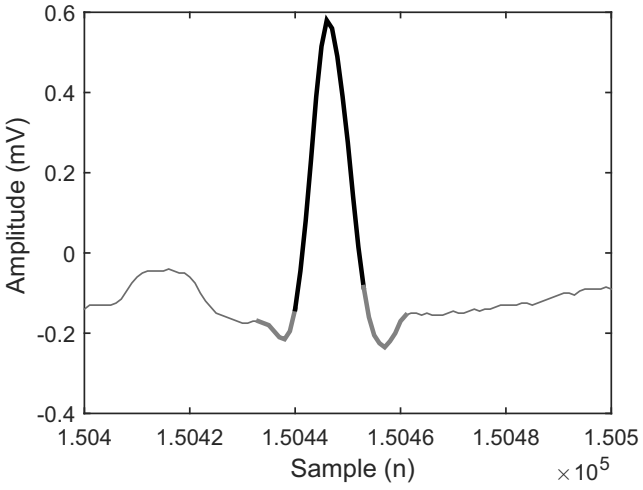

Fig. 3. Composition of QRS complex.

which not only makes vertical scaling difficult but also creates difficulties with horizontal scaling, as the distance ratio from the onset to the R-peak and from the offset to the R-peak is not constant. Resolving this error is a key component of our proposed detection algorithm.

Fig. 4(a) depicts the difficulty of vertical scaling due to baseline fluctuations as seen through changes in the signal amplitude of an ECG, whereas Fig. 4(b) shows the difficulty of horizontal scaling as seen through the nonalignment in the lengths of the left and right regions.

To resolve this problem, we propose separating the primitive into a left and right primitive by using the R-peak as the separation point. From this separation, we can determine the optimal scaling ratios for separated primitives and detect the onset and offset at the endpoints of each divided primitive.

Looking at the left primitive, as shown in (5) and (6), we define the initial primitive signal and N horizontally scaled primitive,

$$P = \{(x_1^P, y_1^P), \cdots, (x_n^P, y_n^P)\}, \quad (5)$$

$$P^j = \{(x_1^{P_j}, y_1^{P_j}), \cdots, (x_{n_j}^{P_j}, y_{n_j}^{P_j})\}. \quad (6)$$

P is the initial primitive signal, P^j is the jth horizontally scaled primitive, and n is the number of the sample data of initial primitives P and P^j. The sample of the P^j signal can be acquired by using linear interpolation, as shown in (7),

$$y_k^{P_j} = y_i^P + (y_{i+1}^P - y_i^P)\frac{x_k^{P_j} - x_i^P}{x_{i+1}^P - x_i^P}, x_k^{P_j} \in (x_i^P, x_{i+1}^P). \quad (7)$$

(x_i^P) and (x_{i+1}^P, y_{i+1}^P) are the data of P from which we can acquire $(x_k^{P_j}, y_k^{P_j})$, which is located between the two.

In general, spline interpolation is better than linear interpolation, and differences become apparent when interpolating a large number of data. However, in this case, the linear interpolation method is relatively acceptable because the variation of the number of data is not large.

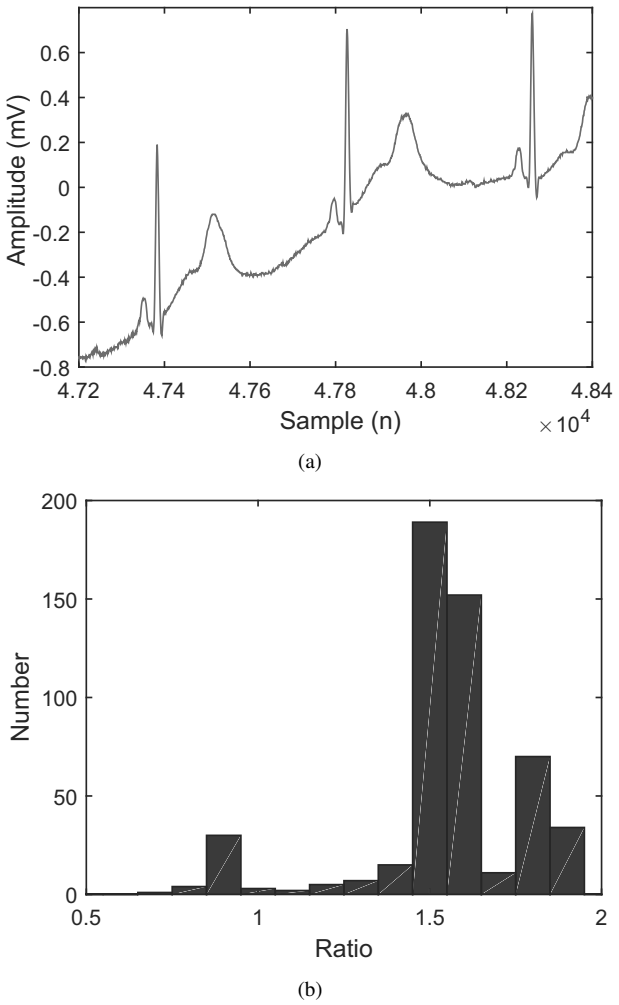

Fig. 4. Variation of the vertical and horizontal ratios of the QRS complex in the QT-DB sel33m: (a) Vertical ratio variations and (b) horizontal ratio histogram.

Next, we apply vertical scaling for P^j to match the original input signal. The original signal, which is matched to P^j data, is defined in (8).

$$S^j = \{(x_1^{S_j}, y_1^{S_j}), \cdots, (x_{n_j}^{S_j}, y_{n_j}^{S_j})\} \quad (8)$$

The number of the data of P^j and S^j is the same as n_j due to linear interpolation, and we can match both endpoints of the two signals by using vertical scaling, as shown in (9),

$$\bar{P^j} = (P^j - y_1^{P_j})\frac{y_n^{S_j} - y_1^{S_j}}{y_n^{P_j} - y_1^{P_j}} + y_1^{S_j}. \quad (9)$$

$y_1^{P_j}$ and $y_1^{S_j}$ are the amplitudes of the left endpoints of P^j and S^j, respectively, and $y_n^{P_j}$ and $y_n^{S_j}$ are the amplitudes of the right endpoints of P^j and S^j, respectively. Through this process, we can acquire the horizontally and vertically scaled primitive denoted as $\bar{P^j}$.

To match the two signals, S^j and $\bar{P^j}$, we next calculate the mean difference of the signals as shown in (10), with the difference denoted as D^j.

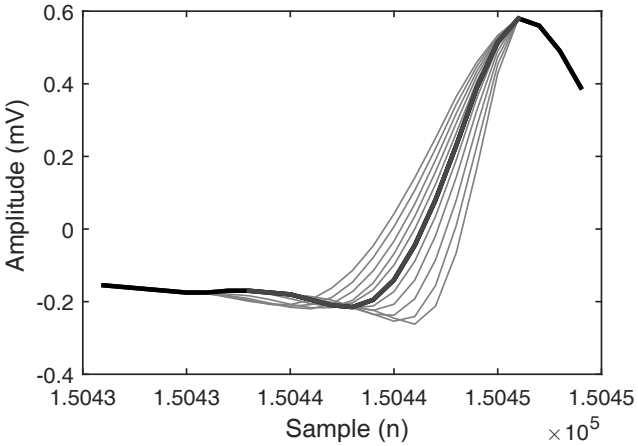

Fig. 5. Adaptive determining of primitive scale.

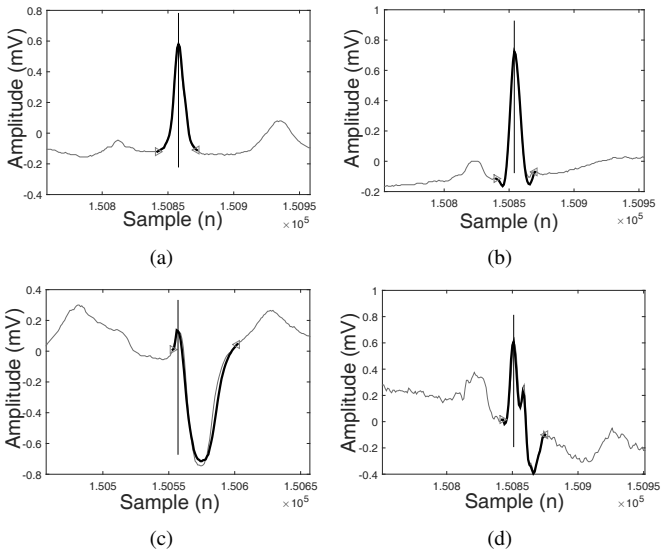

Fig. 6. QRS complex detection result by using primitive.

$$D^j = \frac{\sum_{i=1}^{n_j} |S_i^j - \bar{P_i^j}|}{n_j} \tag{10}$$

Red signals as depicted in Fig. 5 are the $\bar{P^j}$ signals, which were acquired using (5)–(8), whereas the blue signal signifies the mth primitive signal $\bar{P^m}$, which has a minimized mean difference, D^j. For this signal, each endpoint signifies the onset and offset of the QRS complex.

Fig. 6 shows the results of detecting the onset and offset of the QRS complex based on the proposed primitive method of detection. The black signal represents the adaptively scaled primitive when the error is minimized, whereas the red marks represent the detected onset and offset based on the given primitive. As shown in Fig. 6, primitive scaling as detected by the proposed method of this paper can accurately estimate the QRS complex.

D. Improved Algorithm

As depicted in Figs. 6(b), 6(c), and 6(d), the shape of the QRS complex can vary significantly, which suggests that estimating

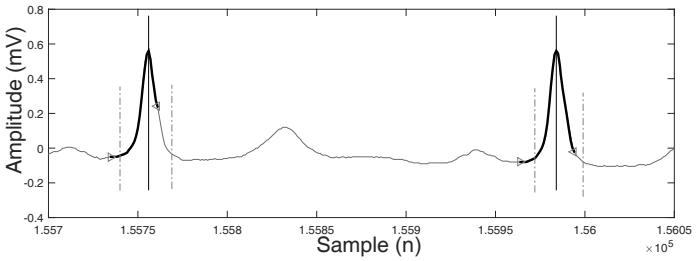

Fig. 7. False detection result of QRS complex.

the onset and offset of the QRS complex with high precision depends on a scaling form in which the average error is minimized. However, in the case of a primitive with a simple shape that lacks a Q-wave and an S-wave, such as the one shown in Fig. 6(a), detection of the QRS complex is relatively straightforward, but the onset and offset points can often be detected incorrectly, as shown in Fig. 7.

As depicted in Fig. 7, the red lines represent the location of the onset and offset of the QRS complex based on the proposed algorithm using data provided in QT-DB, which suggests that detection errors can occur with the proposed algorithm. Additionally, the red triangular markers are the QRS complex onset and offset determined by the primitive. Such false detection errors arise when the primitive form is simple due to distortions in the QRS complex. Hence, an improved algorithm is needed to address this problem.

This paper proposes that the complexity of the QRS complex can be improved by expanding the length of the primitive, then using this expanded baseline region of the primitive for detection. Based on this expanded primitive, the onset and offset of the QRS complex can be detected, and the location of the onset and offset can be readjusted in view of the expanded length of the primitive.

Fig. 8(a) shows the endpoint detection results of the QRS complex onset and offset based on the expanded primitive, whereas Fig. 8(b) shows the readjusted locations of the QRS complex onset and offset based on the length of the extended primitive. The result in Fig. 8 demonstrates that the proposed approach is capable of being an effective approach to mitigate detection errors by the initial version of our proposed primitive-based method, as shown in Fig. 7.

IV. PERFORMANCE ANALYSIS BY SIMULATION

This paper evaluated the proposed algorithm through experiments conducted with QT-DB data as provided by Physionet. The data included information related to the onset, peak, and offset of the P-wave, QRS complex, and T-wave, respectively. In particular, comparative location information was manually recorded for approximately 30 s for each datum as a means to comparatively evaluate the performance of the algorithm. Comparative performance results of the proposed algorithm that detected boundaries of the QRS complex are highlighted through various diagrams, which confirms that the consistency of the proposed algorithm is more reliable than when the location is

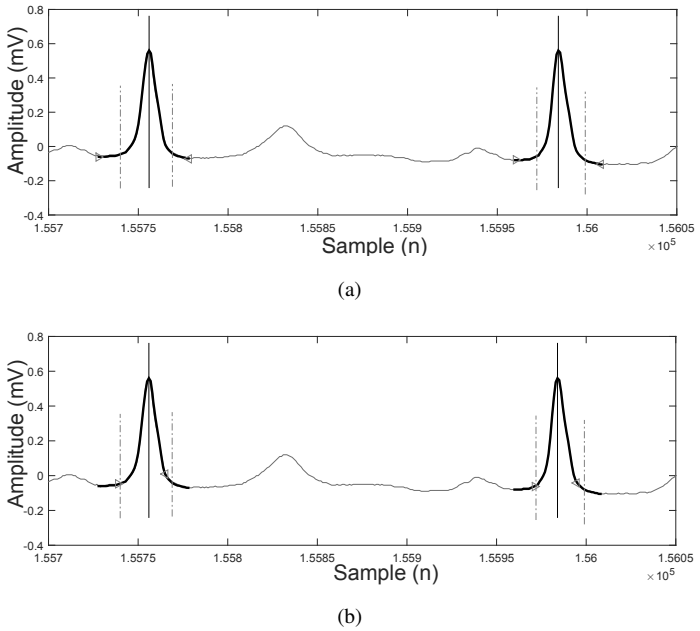

Fig. 8. Improved QRS complex detection algorithm: (a) Detection result of expanding primitive and (b) adjust detection result.

manually measured, as visually depicted through clustering of the QRS complex.

The detected locations of the onset and offset by the proposed algorithm, as shown in Fig. 9, confirm that the endpoints were accurately detected. However, in instances where errors arose in the detection results, the source of the errors was deemed to be from not only the shape of the QRS complex and the algorithm, but also due to the erroneous representation of the location information of the QT-DB data.

Fig. 10 depicts the QRS complex onset and offset location information of sel 17453, as included in the NSRD of the QT-DB. The diagram confirms a relative deviation in the location information of the QRS complex onset and offset.

In contrast, Fig. 11 depicts the normalized clustering of QRS complex data from the NSRD based on the first QRS complex. For each case, the left diagram represents the clustering results of the QRS complex location information recorded manually from the QT-DB, whereas the right diagram represents QRS complex detection results using the proposed primitive.

As shown in Fig. 10, the clustering diagram was unstable due to the erroneous representation of the location information of the QRS complex onset and offset. In contrast, the clustering diagrams of the proposed algorithm were both stable and dense. To evaluate the algorithm, we propose a normalized cross-correlation (NCC) that is calculated between the primitive and QRS complex cluster. NCC is calculated as (11).

$$NCC(i) = \frac{1}{N}\sum_{x=1}^{N}\frac{(C^i(x)-\bar{C^i})(P(x)-\bar{P})}{\sigma_{C^i}\sigma_P}, \qquad (11)$$

where C^i is the ith QRS complex signal of the cluster, P is the primitive signal with length N, and $NCC(i)$ is the normalized

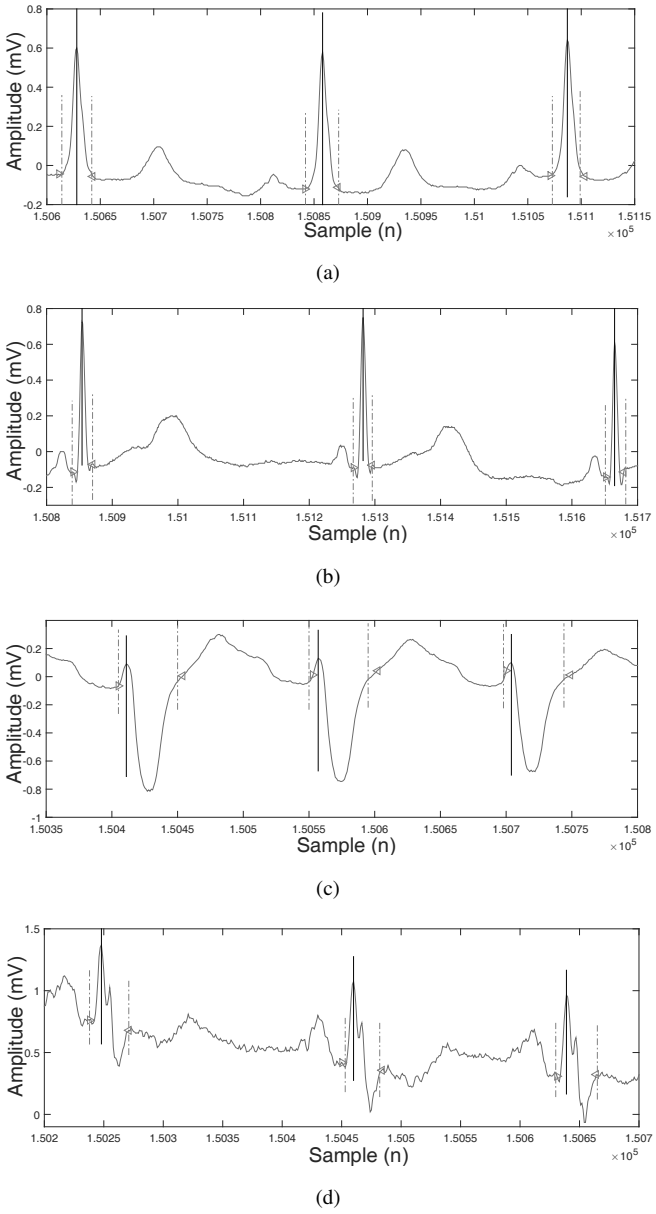

Fig. 9. The result of proposed algorithm: (a) sel 30, (b) sel 33, (c) sel 38, and (d) sel39.

cross-correlation of two signals. $\bar{C^i}$, $\bar{P}$, σ_{C^i}, and σ_P are the mean and standard deviation (STD) of C^i and P, respectively.

In this respect, Fig. 12 shows the difference between the primitive signal and 30 normalized QRS complexes through NCC, based on each datum depicted in Fig. 11.

Fig. 13 shows the NCC distributions of QT-DB and the proposed algorithm. We can clearly see that the proposed algorithm more densely detects the QRS complex.

Table 2 shows the results of calculating the mean and STD of NCC for the data in Fig. 11, which clearly confirms that the detection results of the proposed algorithm are more accurate than QT-DB annotation information.

We summarized the evaluation results in Table 3 to compare between the proposed algorithm and the related works for the entire data set in QT-DB. As shown in Table 3, the accuracy

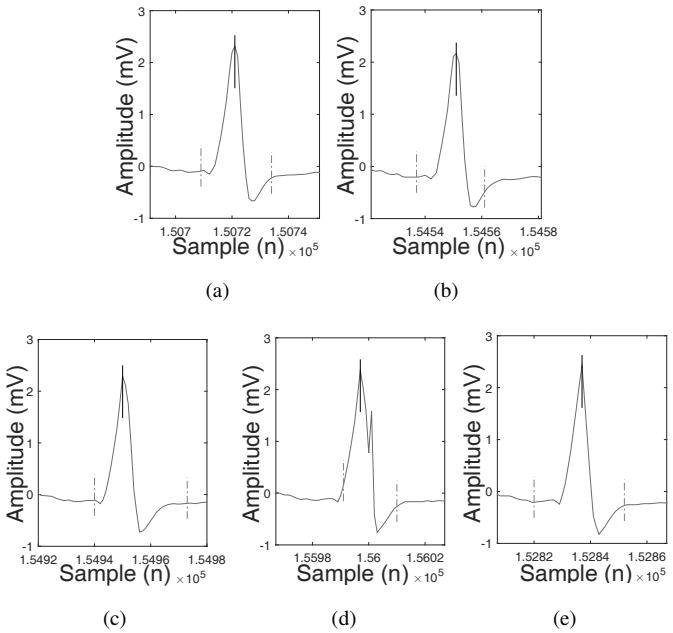

Fig. 10. The error of QRS complex annotation in sel 17,453m.

Table 2. The mean and STD of NCC about NSRD.

Record	QT mean	QT std	P. A. mean	P. A. std
sel 16265	0.9150	0.0430	0.9957	0.0084
sel 16272	0.8427	0.0557	0.9712	0.0211
sel 16273	0.9861	0.0115	0.9958	0.0042
sel 16420	0.9673	0.0356	0.9825	0.0134
sel 16483	0.9675	0.0199	0.9878	0.0105
sel 16539	0.9736	0.0153	0.9865	0.0163
sel 16773	0.9859	0.0143	0.9911	0.0084
sel 16786	0.9693	0.0260	0.9924	0.0067
sel 16795	0.9678	0.0206	0.9879	0.0129
sel 17453	0.9803	0.0177	0.9925	0.0102

Table 3. QRS segmentation performance comparison in the QT-DB.

Method	QRS onset (ms)	QRS offset (ms)
This work	2.21±4.86	-8.81±5.28
Martinez *et al.* [7]	4.6±7.7	0.8±8.7
Martinez *et al.* [8]	-0.2±7.2	2.5±8.9
Madeiro *et al.* [10]	2.85±9.90	2.83±12.26
Laguna *et al.* [16]	-1.1±8.3	-7.2±14.3
Tolerance	6.5	11.6

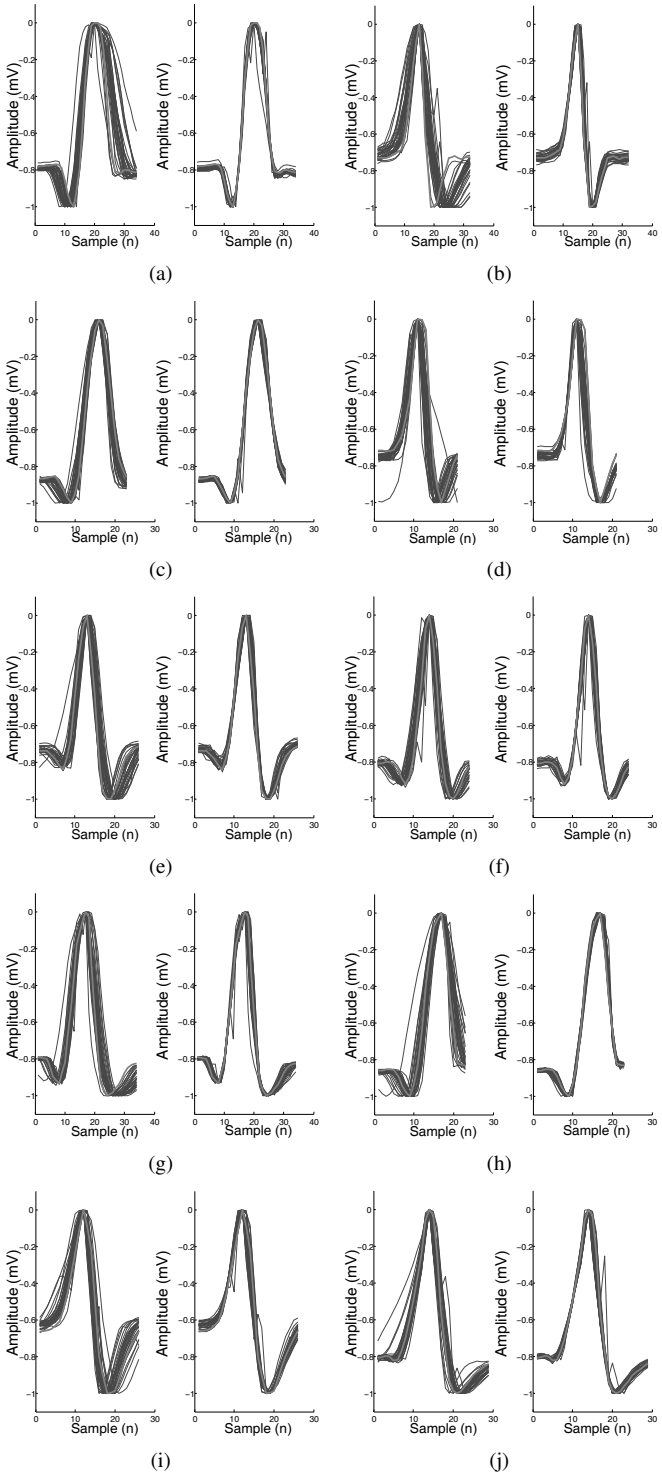

Fig. 11. The comparison of clustering results: (a) sel 16265, (b) sel 16272, (c) sel 16273, (d) sel 16420, (e) sel 16483, (f) sel 16539, (g) sel 16773, (h) sel 16786, (i) sel 16795, and (j) sel 17453.

of the proposed algorithm results are in an acceptable range, which can be regarded as a reasonable method in spite of a small overhead in the proposed signal processing algorithm. In addition, using the proposed algorithm facilitates the reduction of encoded packets of the ECG waves by presenting the repeated QRS wave information using the onset, the offset, and the primitive of QRS. Fig. 14 compares the originally captured signal with the reconstructed signal using primitives in the server-side application, by only sending the extracted primitives instead of transferring entire raw data to the server. The approximated result is very different from the input signal. This result shows that our approach can be applied in small wearable devices with small batteries by reducing the communication overhead.

Recent studies have investigated achieving powerful performance in detecting QRS detection systems [17]. In this study,

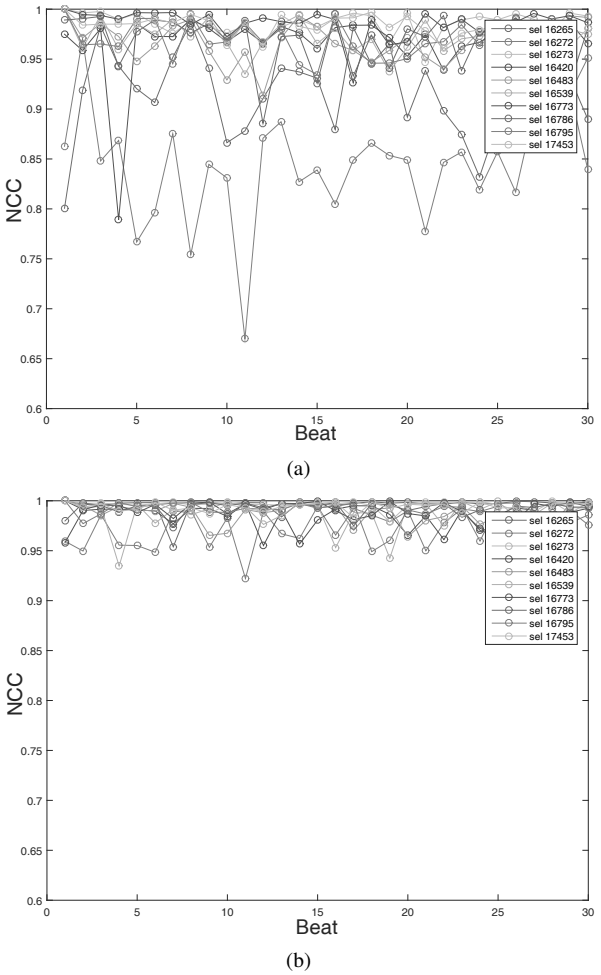

Fig. 12. The result of normalized cross-correlation of Fig. 11: (a) QT-DB and (b) proposed method.

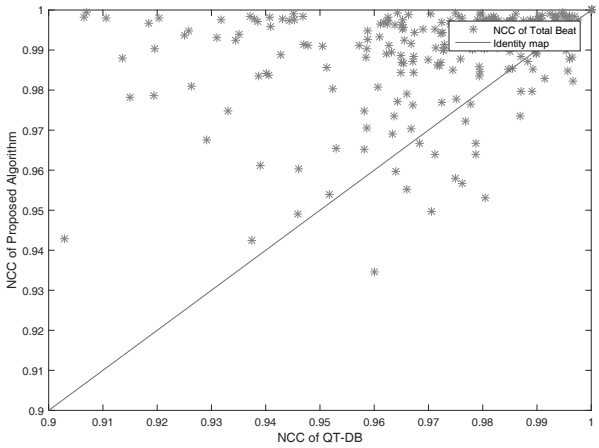

Fig. 13. NCC of total beats of Fig. 11.

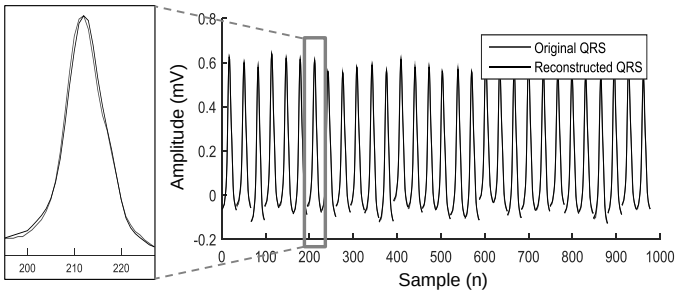

Fig. 14. The signal reconstruction from the encoded QRS data set.

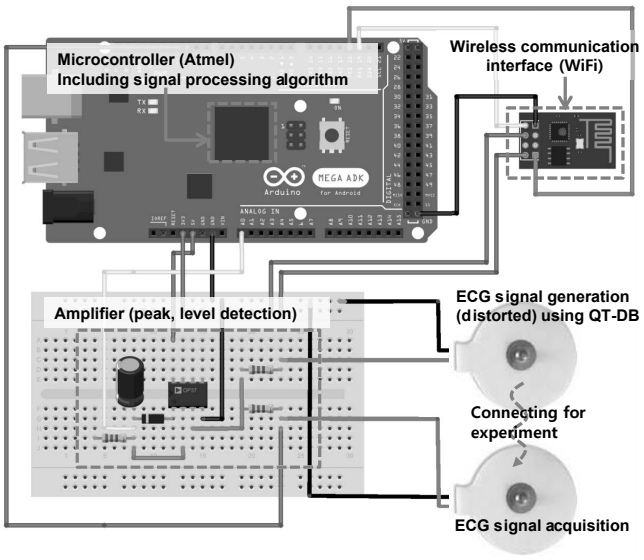

Fig. 15. System implementation using off-the-shelf ATmega2560 microcontroller with the proposed algorithm.

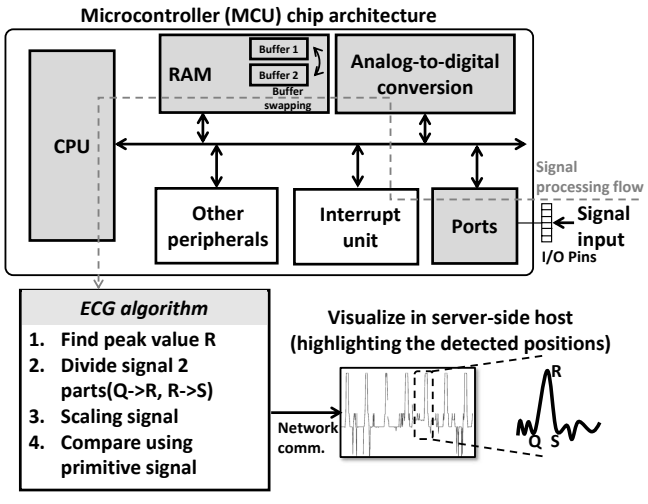

Fig. 16. System architecture and signal processing flow based on off-the-shelf ATmega2560 microcontroller.

we focused on developing a simple and efficient algorithm of detecting QRS from ECG signals based on the primitive, which can be easily applied to tiny signal processing systems built on low-cost commercial off-the-shelf ATmega2560 microcontrollers. We used a peak detector circuit to detect an R-peak position. Fig. 15 shows a prototype of the system implementation for ECG signal acquisition and QRS detection using the proposed algorithm, illustrating that this approach can a feasible solution with small cost in terms of embedded code size of about

6 KB (2.3% of maximum 256 KB) and required data memory of about 2 KB (32% of maximum 8 KB). Fig. 16 describes the systems architecture and signal processing flow based on the ATmega2560 microcontroller. The internally-embedded RAM block performs double buffering for the incoming signal set using the data swapping method to reduce the required amount of data memory. The ECG detection algorithm can be completed with an execution time of 1.2 ms under the 16 MHz CPU clock speed, which is a relatively low overhead of the computation cost compared to the signal acquisition time of 0.8–1.2 s.

Based on the experiments for various cases in the QT-DB, we identified the limitation of the current study, which is that the proposed method can be only applied for similar signals with the expected primitives. This is due to the fact that the proposed algorithm tries to effectively detect primitives for the specific regions of the signals. In this study, we proposed a simple and reasonably accurate algorithm using primitives in matching the ECG signal, so that it can be easily integrated into tiny microcontroller-based signal processing systems. In future studies, improvement of the algorithm for exceptional cases of various ECG signals is needed.

V. CONCLUSION

This paper has proposed a method for detecting the onset and offset of the QRS complex based on the morphological features of the QRS complex, such as the periodically repeated waveform. The proposed algorithm matches the adaptively scaled primitive considering the vertical and horizontal asymmetric areas to the right and left of the baseline fluctuations and the heartbeat, which allows for the detection of the onset and offset of the QRS complex based on the scaled primitive. Additionally, the proposed algorithm extends the length of the primitive to increase the complexity of the QRS complex and the detection accuracy of the onset and offset endpoints for the case of a simple QRS complex that lacks a Q-wave and S-wave. Finally, the proposed algorithm confirmed that the QRS complex detection results are more accurate than the manually entered location information, based on comparisons between the proposed algorithm and manually entered location information from the QT-DB.

REFERENCES

[1] R. J. Huszar, *Basic dysrhythmias: Interpretation & management*. Mosby Jems/Elsevier, 2007.

[2] H. Chan *et al.*, "Continuous and Online Analysis of Heart Rate Variability," *J. Medical Eng. & Tech.*, vol. 29, no. 5, pp. 227–234, 2005.

[3] G. D. Clifford, F. Azuaje, and P. McSharry, *Advanced Methods And Tools for ECG Data Analysis*. Norwood, MA, USA: Artech House, Inc., 2006.

[4] B. M. Oussama, B. M. Saadi, and H. S. Zine-Eddine, "Extracting features from ECG and respiratory signals for automatic supervised classification of heartbeat using neural networks," *Asian J. Inform. Tech.*, vol. 14, no. 2, pp. 53–59, 2015.

[5] J. Pan and W. J. Tompkins, "A real-time QRS detection algorithm," *IEEE Trans. Biomed. Eng.*, vol. BME-32, pp. 230–236, Mar. 1985.

[6] M. E. Nygårds and L. Sörnmo, "Delineation of the QRS complex using the envelope of the E.C.G.," *Medical Biological Eng. Computing*, vol. 21, no. 5, pp. 538–547, 1983.

[7] J. P. Martinez, R. Almeida, S. Olmos, A. P. Rocha, and P. Laguna, "A wavelet-based ECG delineator: Evaluation on standard databases," *IEEE Trans. Biomed. Eng.*, vol. 51, pp. 570–581, Apr. 2004.

[8] A. Martinez, R. Alcaraz, and J. J. Rieta, "Application of the phasor transform for automatic delineation of single-lead ECG fiducial points," *Physiological Measurement*, vol. 31, no. 11, p. 1467, 2010.

[9] A. I. Manriquez and Q. Zhang, "An algorithm for robust detection of QRS onset and offset in ECG signals," in *Proc. CinC*, Sept. 2008, pp. 857–860.

[10] J. P. Madeiro, P. C. Cortez, J. A. Marques, C. R. Seisdedos, and C. R. Sobrinho, "An innovative approach of QRS segmentation based on first-derivative, Hilbert and wavelet transforms," *Medical Eng. & physics*, vol. 34, no. 9, pp. 1236–1246, 2012.

[11] T. H. Kim, S. Y. Kim, J. H. Kim, B. J. Yun, and K. H. Park, "Curvature based ECG signal compression for effective communication on WPAN," *J. Commun. Netw.*, vol. 14, pp. 21–26, Feb. 2012.

[12] P. Laguna, R. G. Mark, A. Goldberg, and G. B. Moody, "A database for evaluation of algorithms for measurement of QT and other waveform intervals in the ECG," in *Proc. CinC*, Sept. 1997, pp. 673–676.

[13] G. B. Moody and R. G. Mark, "The MIT-BIH arrhythmia database on CD-ROM and software for use with it," in *Proc. CinC*, Sept. 1990, pp. 185–188.

[14] A. Taddei *et al.*, "The European ST-T database: Development, distribution, and use," in *Proc. CinC*, Sept. 1990, pp. 177–180.

[15] A. I. Manriquez and Q. Zhang, "An algorithm for QRS onset and offset detection in single lead electrocardiogram records," in *Proc. IEEE EMBC*, Aug. 2007, pp. 541–544.

[16] P. Laguna, R. JanÃl', and P. Caminal, "Automatic detection of wave boundaries in multilead ECG signals: Validation with the CSE database," *Compt. Biomedical Research*, vol. 27, no. 1, pp. 45–60, 1994.

[17] D. B. Saadi *et al.*, "Automatic real-time embedded QRS complex detection for a novel patch-type electrocardiogram recorder," *IEEE J. Translational Eng. Health Medicine*, vol. 3, pp. 1–12, 2015.

Seungmin Lee received B.S. and M.S. degrees in Mathematics from Kyungpook National University (KNU), in Daegu, Korea in 2010 and 2012, respectively. He expanded his research topics to the bio-inspired signal processing algorithm and electronics systems. He is currently pursuing a Ph.D. degree in Electronics Engineering at KNU. His research interest includes signal processing, image processing, bio-inspired signal processing, and compact system implementation.

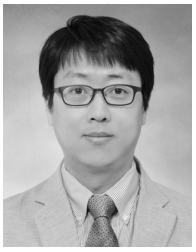

Daejin Park received his B.S. degree in Electronics Engineering from Kyungpook National University, in Daegu, Korea in 2001, and his M.S. degree and Ph.D. degree in Electrical Engineering from the Korea Advanced Institute of Science and Technology (KAIST), Daejeon, Korea, in 2003 and 2014, respectively. He was a Research Engineer in designing high performance signal processors at SK Hynix Semiconductor, Samsung Electronics, for over 12 years from 2003 to 2014. He has explored the accelerated signal processor architecture and low-power chip implementation with custom-designed software algorithm optimization. Dr. Park is a Full-time Professor with the School of Electronics Engineering at Kyungpook National University, in Daegu, Korea.

Kil Houm Park He received his B.S. degree in Electronics Engineering from Kyungpook National University of Daegu, Korea, in 1982. He received his M.S. and his Ph.D. degree in Electrical Engineering from Korea Advanced Institute of Science and Technology (KAIST), in Korea, in 1984 and 1990, respectively. He is now a Full-time Professor at Kyungpook National University in Korea. He has widely published studies in the areas of computer vision, image processing, ECG signal processing, and signal compression.